

Discontinuous Shear Thickening of a Moderately Dense Inertial Suspension of Hydrodynamically Interacting Frictionless Soft Particles: Some New Findings

Satoshi Takada*

*Department of Mechanical Systems Engineering and Institute of Engineering,
Tokyo University of Agriculture and Technology, 2-24-16 Naka-cho, Koganei, Tokyo 184-8588, Japan*

Kazuhiro Hara†

*Department of Industrial Technology and Innovation, Tokyo University of Agriculture and Technology,
2-24-16 Naka-cho, Koganei, Tokyo 184-8588, Japan*

Hisao Hayakawa‡

*Yukawa Institute for Theoretical Physics, Kyoto University,
Kitashirakawa Oiwakecho, Sakyo-ku, Kyoto 606-8502, Japan*

(Dated: August 1, 2022)

We demonstrate that discontinuous shear thickening (DST) can take place even in a moderately dense inertial suspension of hydrodynamically interacting frictionless soft particles. The results which demonstrate this fact are obtained using the Lubrication-Friction Discrete Element Method. Our simulation indicates that DST can be observed for lower densities if the inertia of suspended particles and their softness are both of a marked nature. We also confirm that the DST behavior is effectively approximated by the kinetic theory under these conditions without consideration of hydrodynamic interactions.

Introduction.— Discontinuous shear thickening (DST) is a process, whereby the viscosity of a dense suspension changes abruptly at a certain critical shear rate [1–4]. The normal stress difference also changes abruptly at the same time [5, 6]. DST is observed in suspensions of solid particles in liquid media, and also in frictional dry granular materials [7], where it is closely related to the phenomenon of shear jamming [8–12]. DST is thus of industrial importance, for the design and performance of such apparatus such as sporting equipment [13], traction controls [14], and protective vests [15] as well as materials handling in general. DST also attracts much interest among physicists as an instructive example of a nonequilibrium phase transition. Therefore, the correct physical understanding of DST is both of theoretical interest and a key requirement of the improved design of industrial applications based on densely packed particles.

The physical origin of DST is still the subject of debate. At present, it seems as though the most likely origin of DST lies in inter-particle frictional forces [4, 7, 16, 17]. Other potential causal mechanisms for DST such as order-disorder transition [18–20], and hydrodynamic clusters [1, 21–26] have also been proposed.

It is known that a DST-like phenomenon caused by the ignited-quenched transition exists in inertial suspensions; a model of aerosols has been developed in which collisions between particles play an important role [27–29]. There are also several theoretical studies of inertial suspensions consisting of hard-core frictionless particles based on the

kinetic theory, that is, without hydrodynamic interactions between particles [30–40]. These theoretical studies indicate that DST or the ignited-quenched transition becomes the continuous shear thickening if the volume fraction φ is larger than a few percent [32, 36, 39, 40]. This behavior is completely different from the DST commonly observed in colloidal suspensions, where DST can be observed only in dense suspensions.

In this Letter, we demonstrate the occurrence of DST and the ignited-quenched transition when hydrodynamically interacting particles are soft, frictionless, and in moderately dense concentrations. This finding may be regarded as a new mechanism for DST in moderately dense suspensions. In earlier work, we have reported a complementary analysis based on the kinetic theory of moderately dense inertial suspensions for frictionless soft particles without hydrodynamic interaction [41]; this work is based on an extension of the kinetic theory of dilute inertial suspensions [42]. Thus, clarifying the role of hydrodynamic interactions among particles is also a motivation of our present study.

Langevin model.— We consider N monodisperse frictionless soft particles (each particle of mass m and diameter d), which are suspended in a fluid and are confined in a three-dimensional cubic box with the linear size L . We assume that the contact force between particles is described by the harmonic potential

$$U(r) = \frac{\varepsilon}{2} \left(1 - \frac{r}{d}\right)^2 \Theta\left(1 - \frac{r}{d}\right), \quad (1)$$

where r is the inter-particle distance and ε is the energy scale to characterize the repulsive interaction, and $\Theta(x)$, defined as $\Theta(x) = 1$ ($x \geq 0$) and 0 ($x < 0$) is the step function. Although clustering effects caused by attractive interactions between particles cannot be ignored in real-

* e-mail: takada@go.tuat.ac.jp

† e-mail: hara@st.go.tuat.ac.jp

‡ e-mail: hisao@yukawa.kyoto-u.ac.jp

istic situations, such effects are suppressed if particles are charged [43–45]. Moreover, particles are also prevented from clustering if the temperature is high enough [30, 46–48].

The equation of motion of the suspended particle i (its position \mathbf{r}_i) under simple shear with the shear rate $\dot{\gamma}$ is given by

$$\frac{d\mathbf{p}_i}{dt} = \sum_{j \neq i} \mathbf{F}_{ij} - \sum_j \overleftrightarrow{\zeta}_{ij} \mathbf{p}_j + \boldsymbol{\zeta}_i^{\text{Sh}} + \boldsymbol{\xi}_i, \quad (2)$$

where we have introduced the peculiar momentum $\mathbf{p}_i \equiv m(\mathbf{v}_i - \dot{\gamma} y_i \hat{\mathbf{e}}_x)$ with the unit vector $\hat{\mathbf{e}}_x$ parallel to the x direction and the velocity \mathbf{v}_i of the i -th particle, $\mathbf{F}_{ij} \equiv -\partial U(r_{ij})/\partial \mathbf{r}_{ij}$ is the inter-particle force between the i -th and j -th particles with $\mathbf{r}_{ij} \equiv \mathbf{r}_i - \mathbf{r}_j$ and $r_{ij} \equiv |\mathbf{r}_{ij}|$.

The terms containing $\overleftrightarrow{\zeta}_{ij}$ and $\boldsymbol{\zeta}_i^{\text{Sh}}$ in Eq. (2) originate from the hydrodynamic force acting on the i -th particle. If smooth particles are embedded in a Stokes fluid, the particles cannot collide with each other because the lubrication force between contacting particles pushes them apart, hydrodynamically, before they make contact [49–53]. We note that previous studies of colloidal suspensions have ignored the effects of inertia in the equation of motion. Therefore, it is important to clarify the role of both hydrodynamic interactions and inertia effects on the rheology of the system we are modeling [54]. For this purpose, we focus on situations in which the fluid motion can be described by the Stokes equation, and in which, therefore, the resistance matrix $\overleftrightarrow{\zeta}_{ij}$ depends only on the positions of the i -th and j -th particles. Then, we adopt the Lubrication-Friction Discrete Element Method (LF-DEM) which considers only the short-range lubrication force between particles [4, 48]. Such a simplification, whereby we ignore long-range hydrodynamic interactions, may be justified in relatively dense particle concentrations.

Within the framework of the LF-DEM the resistance matrix $\overleftrightarrow{\zeta}_{ij}$ in the Stokes flow is expressed as [48, 52, 55]

$$\zeta_{ij,\alpha\beta} = \begin{cases} 3\pi \frac{\eta_0 d_H}{m} \delta_{\alpha\beta} + \sum_{k \neq i} \frac{1}{m} A_{ik,\alpha\beta}^{(11)} \Theta(r_c - r_{ik}) & (i = j) \\ -\frac{1}{m} A_{ij,\alpha\beta}^{(11)} \Theta(r_c - r_{ij}) & (i \neq j) \end{cases}, \quad (3)$$

where η_0 is the viscosity of the solvent, $r_c \equiv d_H(1 + \delta)$ is the cutoff length of the lubrication force with the hydrodynamic diameter d_H (which is $d_H \leq d$), and $A_{ij,\alpha\beta}^{(11)}$ is given by Refs. [55, 56]. Although smooth hard-core particles are not allowed to contact each other [49–53], the LF-DEM does allow contact between rough particles, and so we introduce the roughness parameter $\delta \equiv (d - d_H)/d_H$ [4, 12, 48]. This parameter equates to a simplified description of dimples located on the surface of particles. Previous papers have adopted $\delta = 0.05$ [4, 12, 48], but we are free to choose larger or smaller values of δ . Similarly, the vector $\boldsymbol{\zeta}_i^{\text{Sh}}$ is the contribution from the shear flow due

to the lubrication force:

$$\zeta_{i,\alpha}^{\text{Sh}} = 2\eta_0 \dot{\gamma} \sum_j \tilde{G}_{ij,xy\alpha}^{(11)}, \quad (4)$$

where $\tilde{G}_{ij,xy\alpha}^{(11)}$ is presented in Refs. [55, 57].

The noise parameter $\boldsymbol{\xi}_i(t) = \xi_{i,\alpha}(t) \hat{\mathbf{e}}_\alpha$ satisfies the fluctuation-dissipation relation:

$$\langle \boldsymbol{\xi}_i(t) \rangle = \mathbf{0}, \quad \langle \xi_{i,\alpha}(t) \xi_{j,\beta}(t') \rangle = 2mT_{\text{env}} \zeta_{ij,\alpha\beta} \delta(t - t'), \quad (5)$$

where $\langle \cdot \rangle$ expresses the average over the noise and T_{env} is the environmental (solvent) temperature. Note that the resistance matrix $\overleftrightarrow{\zeta}_{ij}$ is not diagonal if hydrodynamic interaction exists between the particles. The implementation of the noise parameter $\boldsymbol{\xi}_i(t)$ satisfying Eq. (5) is explained in Ref. [55]. We also note that $\boldsymbol{\zeta}_i^{\text{Sh}}$ in Eq. (2) expresses the hydrodynamic force in the presence of the shear flow, which is proportional to the shear rate $\dot{\gamma}$ [49–53]. Now, let us introduce two dimensionless parameters for later convenience:

$$\varepsilon^* \equiv \frac{\varepsilon}{md^2 \zeta^2}, \quad \xi_{\text{env}} \equiv \sqrt{\frac{T_{\text{env}}}{m}} \frac{1}{d\zeta}, \quad (6)$$

where $\zeta \equiv 3\pi\eta_0 d/m$ is the Stokesian drag acting on a sphere.

The assumptions behind Eqs. (2) and (5) are summarized as follows. (i) Particles are suspended in a fluid in which the motion of the particles is agitated by white Gaussian noise as in Eq. (5), (ii) the environmental temperature T_{env} is independent of the motion of the suspended particles, (iii) the hydrodynamic interactions among the particles are only described by the lubrication force, and (iv) the effects of gravity can be ignored. Although gravitational sedimentation plays some role in aerosols, such an effect is negligible within the observation time for small, suspended particles [28, 29]. In addition, inertial suspension can be regarded as a model of a colloidal suspension, in which the sedimentation effect is negligible and the hydrodynamic interactions among particles play important roles.

We adopt SLLOD dynamics [58, 59] to simulate shear flow under the Lees-Edwards boundary condition [60]. As far as we have checked, the uniform flow is stable once the system reaches a steady state.

Rheology.— In this system, the stress tensor is given by

$$\sigma_{\alpha\beta} = \frac{1}{NL^3} \sum_i \left\langle \left(-mv_{i,\alpha} v_{i,\beta} - \frac{1}{2} \sum_{j \neq i} r_{ij,\alpha} F_{ij,\beta}^{(\text{el})} + \bar{\sigma}_{i,\alpha\beta}^{\text{St}} + \frac{1}{2} \sum_{j \neq i} \bar{\sigma}_{ij,\alpha\beta}^{\text{H}} \right) \right\rangle, \quad (7)$$

$\bar{\sigma}_{i,\alpha\beta}^{\text{St}}$ is given by [52]

$$\bar{\sigma}_{i,\alpha\beta}^{\text{St}} = \frac{5}{12} \pi d_H^3 \eta_0 \dot{\gamma} (\delta_{\alpha x} \delta_{\beta y} + \delta_{\alpha y} \delta_{\beta x}), \quad (8)$$

and the hydrodynamic stress $\bar{\sigma}_{ij,\alpha\beta}^H$ between the i -th and the j -th particles is given by [52]

$$\bar{\sigma}_{ij,\alpha\beta}^H = -2\eta_0 G_{ij,\alpha\beta\gamma}^{(11)} V_{ij,\gamma} + 2\eta_0 \dot{\gamma} M_{ij,\alpha\beta}^{(1)}, \quad (9)$$

with $\mathbf{V}_i \equiv \mathbf{v}_i - \dot{\gamma} y_i \hat{\mathbf{e}}_x$ and $V_{ij,\gamma}$ is γ component of $\mathbf{V}_i - \mathbf{V}_j$. The explicit expressions of $G_{ij,\alpha\beta\gamma}^{(11)}$ and $M_{ij,\alpha\beta}^{(1)}$ are presented in Refs. [55, 61].

Let us introduce the Peclet number Pe defined as [62]

$$Pe \equiv \frac{3\pi\eta_0 d^3}{4T_{\text{env}}} \dot{\gamma}. \quad (10)$$

Since ξ_{env} introduced in Eq. (6) is proportional to $\sqrt{mT_{\text{env}}/\eta_0^2 d^4}$, as shown in Eq. (6), ξ_{env} increases as the inertia becomes important. Using $\dot{\gamma}^*$, we introduce the dimensionless viscosity η^* as

$$\eta^* \equiv \frac{\sigma_{xy}}{nT_{\text{env}}Pe}. \quad (11)$$

We examine $N = 1000$ and 10 ensemble averages in the simulations. We control Pe , ξ_{env} , ε^* , and δ in the range $0.25 \leq Pe \leq 25$, $1 \leq \xi_{\text{env}} \leq 10^2$, $10^2 \leq \varepsilon^* \leq 10^8$, and $0.02 \leq \delta \leq 0.25$, respectively.

Figure 1 shows how the scaled viscosity $\tilde{\eta} \equiv \eta^*/\eta_a$ and the dimensionless temperature $\theta \equiv T/T_{\text{env}}$ depend on Pe with fixed values of $\varphi (= \pi N d^3 / (6L^3)) = 0.30$, $\varepsilon^* = 10^4$, and $\xi_{\text{env}} = 1.0$ for various δ , where we have introduced the kinetic temperature $T \equiv \sum_{i=1}^N \langle m_i \mathbf{V}_i^2 \rangle / (3N)$ and the empirical expression of the apparent viscosity η_a in the low shear limit $\eta_a = 1 + (5/2)\varphi + 4\varphi^2 + 42\varphi^3$ [63]. Note that we do not have any theoretical result for η_a until $O(\varphi^3)$ as far as we have been able to ascertain, though the expression until $O(\varphi^2)$ is well known for hard-core suspensions [64]. Figure 2 is the corresponding result for $\varphi = 0.40$ with $\delta = 0.05$ and $\delta = 0.02$. Figures 1(a) and 2(a) exhibit remarkable results, in which DST can be observed around $Pe = 10$. It is noteworthy that DST is observed even for $\delta = 0.02$ (Figs. 1 (a) and 2(a)), though the discontinuous jump of the viscosity is enhanced for larger values of δ . Although the quantitative agreement between the kinetic theory without consideration of hydrodynamic interactions [41] and hydrodynamic simulation is poor for $\varphi = 0.40$ (see Fig. 2(a)), the kinetic theory captures the qualitative behavior of the DST. Moreover, the agreement between the theory and simulation is reasonable for $\varphi = 0.30$ (Fig. 1 (a)). We note that the results of the simulation based on the LF-DEM approach the theoretical prediction reported in Ref. [41] as δ increases, though we have used the empirical expression for η_a . Figures 1(b) and 2(b) indicate that these DSTs are caused by the ignited-quenched transition.

Thus, we have confirmed that DST and the ignited-quenched transition of inertial suspensions for soft and frictionless particles can survive even if hydrodynamic interactions between particles exist. We have also confirmed the relevance of the kinetic theory developed in Ref. [41] to describe the suspensions with hydrodynamic interactions.

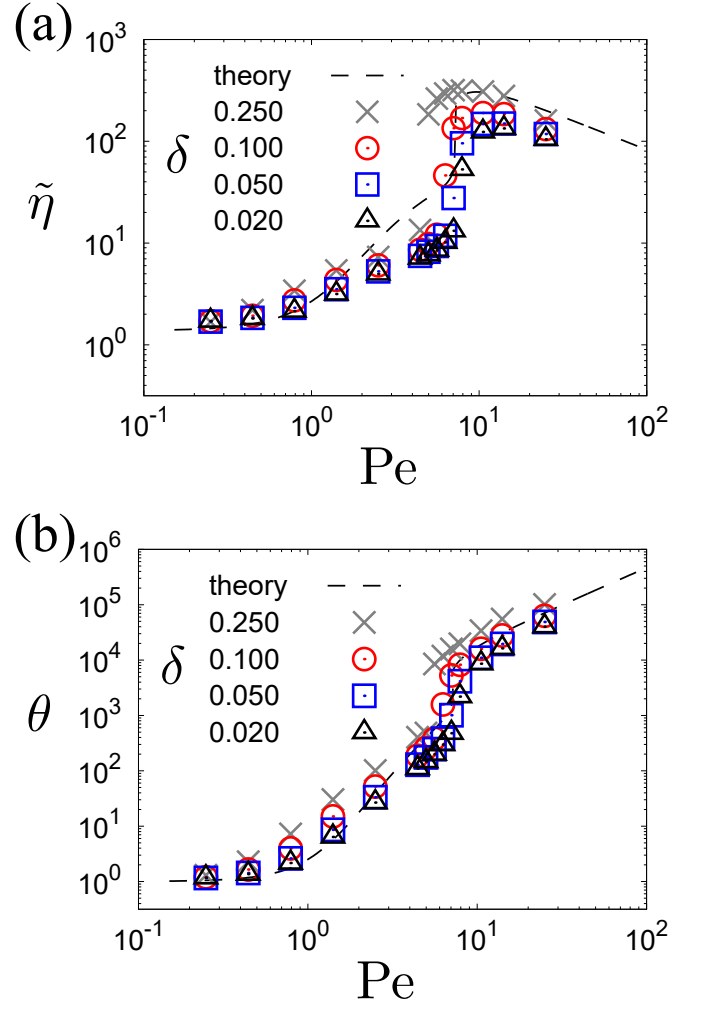


FIG. 1. Plots of (a) $\tilde{\eta}$ and (b) θ against Pe for $\delta = 0.02$ (open circles), 0.05 (open squares), 0.10 (open triangles), and 0.25 (crosses) with fixed values of $\varphi = 0.30$, $\varepsilon^* = 10^4$, and $\xi_{\text{env}} = 1.0$. The dashed line represents the prediction of the kinetic theory in Ref. [41].

Figure 3(a) is the plot of $\tilde{\eta}$ against Pe for various ξ_{env} with fixed values of $\delta = 0.05$ and $\varphi = 0.40$. We verify that DST still persists for $\xi_{\text{env}} = 10$ but disappears around $10 \lesssim \xi_{\text{env}} \lesssim 20$. Figure 3(b) is the plot of $\tilde{\eta}/\varepsilon^{*4/3}$ against Pe for various ε^* with fixed values of $\delta = 0.05$ and $\varphi = 0.40$. Except for the case of $\varepsilon^* = 10^2$, $\tilde{\eta}$ exhibits DST. As the softness parameter ε^* increases, the upper branch also increases (see Fig. 3(b)). In accordance with Ref. [41] and as shown in Figs. 3(b) and (c), the viscosity in the upper branch is scaled as $\tilde{\eta}/\varepsilon^{*4/3}$ except for $\varepsilon^* = 10^2$. Thus, we conclude that DST with frictionless soft particles can be observed for systems with $\xi_{\text{env}} \leq 20$ and $\varepsilon^* \geq 10^4$.

Concluding remarks.— In this Letter, we have successfully demonstrated the existence of DST-like changes in viscosity and kinetic temperature for moderately dense inertial suspensions composed of frictionless soft particles using the LF-DEM. The kinetic theory without consid-

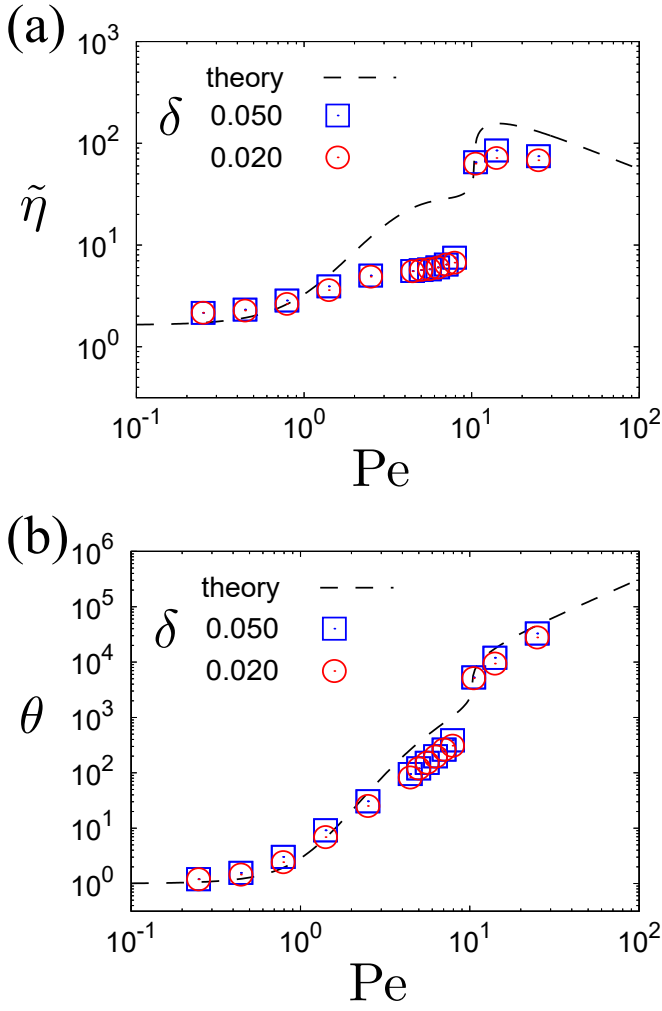


FIG. 2. Plots of (a) $\tilde{\eta}$ and (b) θ against Pe for $\delta = 0.05$ (open squares) and $\delta = 0.02$ (open circles) with fixed values of $\varphi = 0.40$, $\varepsilon^* = 10^4$, and $\xi_{\text{env}} = 1.0$. The dashed line represents the prediction of the kinetic theory in Ref. [41].

eration of hydrodynamic interaction effectively describes the discontinuous behaviors of both viscosity and kinetic temperature. Our results also reveal a new mechanism for DST caused by the ignited-quenched transition for frictionless soft particles.

It is difficult to observe the simultaneously large and discontinuous changes of η^* and θ obtained in our model if the solvent is a liquid. Indeed, if the kinetic temperature in the ignited phase becomes 10^6 times larger than that in the quenched phase, the liquid in the ignited phase might be evaporated because of the strong stirring effect of suspended particles, though our model does not include such effects. Even if we consider particles suspended in a gas, it might be difficult to avoid the melting of solid particles. Nevertheless, an indication of the existence of DST-like changes of η^* and θ for frictionless soft particles, even among relatively dense suspensions, is important.

Let us discuss whether this behavior is observable in

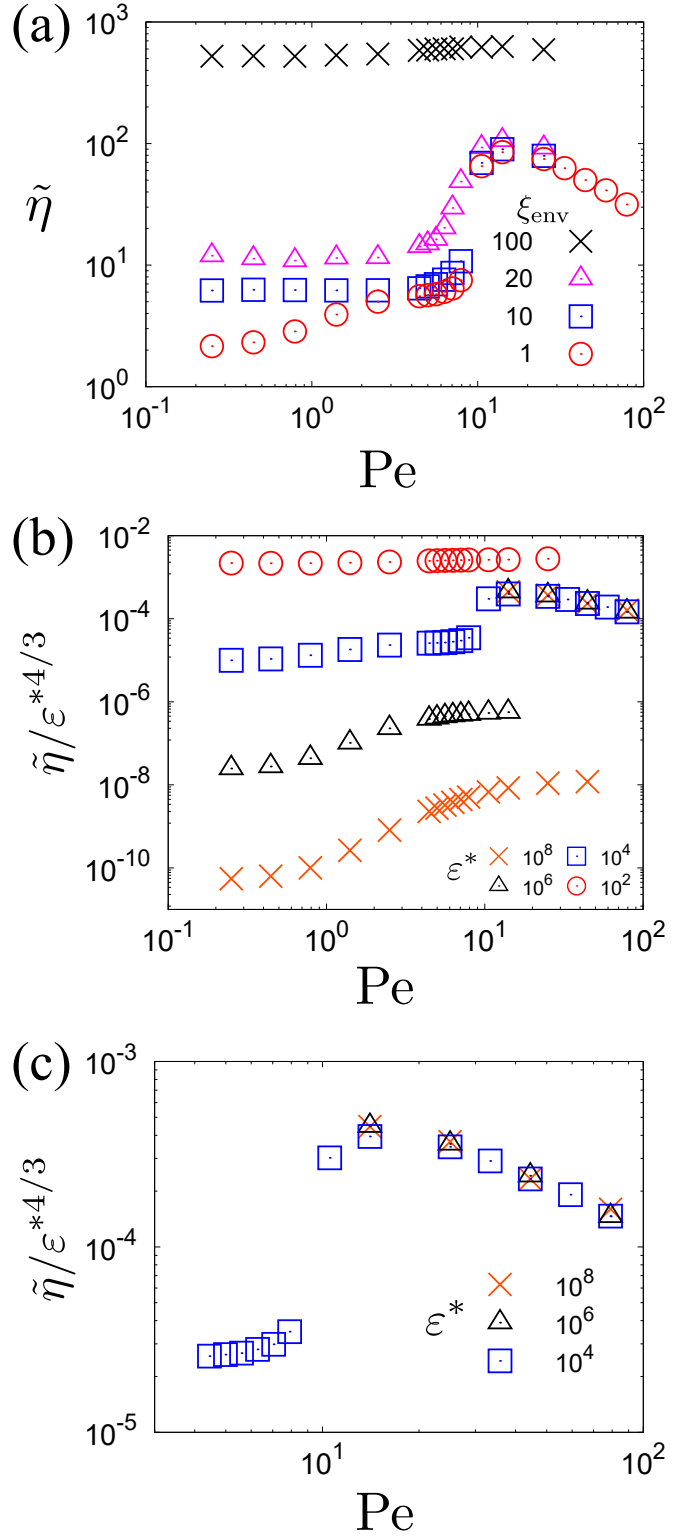


FIG. 3. (a) Plot of $\tilde{\eta}$ against Pe for various ξ_{env} . (b) Plot of $\tilde{\eta}/\varepsilon^{*4/3}$ for various ε^* . Here, we fix (a) $\varepsilon^* = 10^4$ and (b) $\xi_{\text{env}} = 1$, respectively. (c) A detailed view of the high Pe regime of (b). Parameters are fixed as $\varphi = 0.40$ and $\delta = 0.05$.

experiments of colloidal suspensions. Here, let us assume that the diameter, the mass density, and Young's modulus of colloidal particles are given by $d = 2 \times 10^{-6}$ m, $\rho = 10^3$ kg/m³, and $Y = 10$ GPa, and thus, the mass m becomes $m \sim 4 \times 10^{-15}$ kg. When we consider a case when the solvent is water at room temperature, of which the viscosity is $\eta_0 \sim 10^{-3}$ Pa · s, the corresponding drag coefficient becomes $\zeta = 3\pi\eta_0 d/m \sim 5 \times 10^6$ s⁻¹. We can also evaluate $\varepsilon^* \sim 6 \times 10^5 \delta \sim 6 \times 10^3$ with the assumption of $\delta \sim 10^{-2}$ [65]. The value of ε^* is close to that used in Fig. 3. Note that the behavior of the viscosity can be scaled by $\varepsilon^{4/3}$. This means that the DST discussed in this paper can be observed in the region of large Pe. A serious problem exists in the value of ξ_{env} . If we assume that $T_{\text{env}} = 4 \times 10^{-21}$ J corresponding to the room temperature, ξ_{env} becomes about 2×10^{-4} . This value is

much smaller than the critical value ($10 < \xi_{\text{env}}^c < 10^2$) of the absence of the DST, which means that we can expect the existence of the DST. We have verified that the DST still can be observed for realistic values of parameters in the prediction of the kinetic theory [41]. Thus, the observation of such a DST for frictionless small grains which are supposed to be Brownian suspensions is challenging for experimentalists.

Needless to say, it is important to analyze suspensions of frictional grains for larger ε^* corresponding to the typical experimental setup for colloidal suspensions. This will be our forthcoming task.

Acknowledgements.— The authors thank Takeshi Kawasaki, Takashi Uneyama, Michio Otsuki, and Pradipto for their helpful comments. This research was partially supported by Grants-in-Aid from MEXT for Scientific Research (Grant Nos. JP20K14428 and JP21H01006).

-
- [1] N. J. Wagner and J. F. Brady, *Shear thickening in colloidal dispersions*, Phys. Today **62**, 27 (2009).
 - [2] E. Brown and H. M. Jaeger, *Shear thickening in concentrated suspensions: phenomenology, mechanisms and relations to jamming*, Rep. Prog. Phys. **77**, 046602 (2014).
 - [3] C. Ness, R. Seto, and R. Mari, *The Physics of Dense Suspensions*, Ann. Rev. Cond. Mat. Phys. **13**, 97 (2022).
 - [4] R. Seto, R. Mari, J. F. Morris, and M. M. Denn, *Discontinuous Shear Thickening of Frictional Hard-Sphere Suspensions*, Phys. Rev. Lett. **111**, 218301 (2013).
 - [5] H. M. Laun, *Normal stresses in extremely shear thickening polymer dispersions*, J. Non-Newton. Fluid Mech. **54**, 87 (1994).
 - [6] C. D. Cwalina and N. J. Wagner, *Material properties of the shear-thickened state in concentrated near hard-sphere colloidal dispersions*, J. Rheol. **58**, 949 (2014).
 - [7] M. Otsuki and H. Hayakawa, *Critical scaling near jamming transition for frictional granular particles*, Phys. Rev. E **83**, 051301 (2011).
 - [8] D. Bi, J. Zhang, B. Chakraborty, and R. P. Behringer, *Jamming by shear*, Nature **480**, 355 (2011).
 - [9] A. Fall, F. Bertrand, D. Hautemayou, C. Mezière, P. Moucheron, A. Lemaître, and G. Ovarlez, *Macroscopic Discontinuous Shear Thickening versus Local Shear Jamming in Cornstarch*, Phys. Rev. Lett. **114**, 098301 (2015).
 - [10] I. R. Peters, S. Majumdar, and H. M. Jaeger, *Direct observation of dynamic shear jamming in dense suspensions*, Nature **532**, 214 (2016).
 - [11] M. Otsuki and H. Hayakawa, *Shear jamming, discontinuous shear thickening, and fragile states in dry granular materials under oscillatory shear*, Phys. Rev. E **101**, 032905 (2020).
 - [12] Pradipto and H. Hayakawa, *Simulation of dense non-Brownian suspensions with the lattice Boltzmann method: shear jammed and fragile states*, Soft Matter **16**, 945 (2020), [Correction] **18**, 685 (2022).
 - [13] C. Fischer, S. A. Braun, P.-E. Bourban, V. Michaud, C. J. G. Plummer, and J.-A. E. Månson, *Smart Materials and Structures Dynamic properties of sandwich structures with integrated shear-thickening fluids*, Smart Mater. Struct. **15**, 1467 (2006).
 - [14] H. M. Laun, R. Bung, and F. Schmidt, *Rheology of extremely shear thickening polymer dispersions (passively viscosity switching fluids)*, J. Rheol. **35**, 999 (1991).
 - [15] Y. S. Lee, E. D. Wetzal, and N. J. Wagner, *The ballistic impact characteristics of Kevlar® woven fabrics impregnated with a colloidal shear thickening fluid*, J. Mater. Sci. **38**, 2825 (2003).
 - [16] T. Kawasaki and L. Berthier, *Discontinuous shear thickening in Brownian suspensions*, Phys. Rev. E **98**, 012609 (2018).
 - [17] M. Wyart and M. E. Cates, *Discontinuous Shear Thickening without Inertia in Dense Non-Brownian Suspensions*, Phys. Rev. Lett. **112**, 098302 (2014).
 - [18] R. L. Hoffman, *Discontinuous and Dilatant Viscosity Behavior in Concentrated Suspensions. I. Observation of a Flow Instability*, Trans. Soc. Rheol. **16**, 155 (1972).
 - [19] R. L. Hoffman, *Discontinuous and dilatant viscosity behavior in concentrated suspensions. II. Theory and experimental tests*, J. Colloid Interface Sci. **46**, 491 (1974).
 - [20] R. L. Hoffman, *Explanations for the cause of shear thickening in concentrated colloidal suspensions*, J. Rheol. **42**, 111 (1998).
 - [21] M. Wang, S. Jamali, and J. F. Brady, *A hydrodynamic model for discontinuous shear-thickening in dense suspensions*, J. Rheol. **64**, 379 (2020).
 - [22] J. F. Brady and G. Bossis, *The rheology of concentrated suspensions of spheres in simple shear flow by numerical simulation*, J. Fluid Mech. **155**, 105 (1985).
 - [23] J. F. Brady and G. Bossis, *Stokesian Dynamics*, Ann. Rev. Fluid Mech. **20**, 111 (1988).
 - [24] J. Bender and N. J. Wagner, *Reversible shear thickening in monodisperse and bidisperse colloidal dispersions*, J. Rheol. **40**, 899 (1996).
 - [25] J. R. Melrose and R. C. Ball, *Continuous shear thickening transitions in model concentrated colloids—The role of interparticle forces*, J. Rheol. **48**, 937 (2004).
 - [26] R. S. Farr, J. R. Melrose, and R. C. Ball, *Kinetic theory of jamming in hard-sphere startup flows*, Phys. Rev. E **55**, 7203 (1997).

- [27] S. K. Friedlander, *Smoke, Dust and Haze: Fundamentals of Aerosol Dynamics*, 2nd ed. (Oxford Univ. Press, Oxford, 2000).
- [28] D. L. Koch and R. J. Hill, *Inertial Effects in Suspension and Porous-Media Flows*, Ann. Rev. Fluid Mech. **33**, 619 (2001).
- [29] M. Hu, J. Peng, K. Sun, D. Yue, S. Guo, A. Wiedensohler, and Z. Wu, *Estimation of Size-Resolved Ambient Particle Density Based on the Measurement of Aerosol Number, Mass, and Chemical Size Distributions in the Winter in Beijing*, Environ. Sci. Technol. **46**, 9941 (2012).
- [30] H. Hayakawa and S. Takada, *Kinetic theory of discontinuous shear thickening for a dilute gas-solid suspension*, Prog. Theor. Exp. Phys. **2019**, 083J01 (2019).
- [31] H.-W. Tsao and D. L. Koch, *Simple shear flows of dilute gas-solid suspensions*, J. Fluid Mech. **296**, 211 (1995).
- [32] A. S. Sangani, G. Mo. H.-W. Tsao, and D. L. Koch, *Simple shear flows of dense gas-solid suspensions at finite Stokes numbers*, J. Fluid Mech. **313**, 309 (1996).
- [33] D. L. Koch and A. S. Sangani, *Particle pressure and marginal stability limits for a homogeneous monodisperse gas-fluidized bed: kinetic theory and numerical simulations*, J. Fluid Mech. **400**, 229 (1999).
- [34] D. L. Koch and R. J. Hill, *Inertial Effects in Suspension and Porous-Media Flows*, Ann. Rev. Fluid Mech. **33**, 619 (2001).
- [35] V. Garzó, S. Tennetti, S. Subramaniam, and C. M. Hrenya, *Enskog kinetic theory for monodisperse gas-solid flows*, J. Fluid Mech. **712**, 129 (2012).
- [36] S. Saha and M. Alam, *Revisiting ignited-quenched transition and the non-Newtonian rheology of a sheared dilute gas-solid suspension*, J. Fluid. Mech. **833**, 206 (2017).
- [37] M. Alam, S. Saha, and R. Gupta, *Unified theory for a sheared gas-solid suspension: from rapid granular suspension to its small-Stokes-number limit*, J. Fluid Mech. **870**, 1175 (2019).
- [38] S. Saha and M. Alam, *Burnett-order constitutive relations, second moment anisotropy and co-existing states in sheared dense gas-solid suspensions*, J. Fluid Mech. **887**, 25 (2020).
- [39] H. Hayakawa, S. Takada, and V. Garzó, *Kinetic theory of shear thickening for a moderately dense gas-solid suspension: From discontinuous thickening to continuous thickening*, Phys. Rev. E **96**, 042903 (2017), [Erratum] **101**, 069904(E) (2020).
- [40] S. Takada, H. Hayakawa, A. Santos, and V. Garzó, *Enskog kinetic theory of rheology for a moderately dense inertial suspension*, Phys. Rev. E **102**, 022907 (2020).
- [41] S. Takada, K. Hara, and H. Hayakawa, *Kinetic theory of discontinuous shear thickening of a moderately dense inertial suspension of frictionless soft particles*, arXiv:2207.05752.
- [42] S. Sugimoto and S. Takada, *Two-Step Discontinuous Shear Thickening of Dilute Inertial Suspensions Having Soft-Core Potential*, J. Phys. Soc. Jpn. **89**, 084803 (2020), [Addendum] **89**, 127001 (2020).
- [43] B. Derjaguin and L. D. Landau, *Theory of the stability of strongly charged lyophobic sols and of the adhesion of strongly charged particles in solutions of electrolytes*, Acta Physicochim. URSS **14**, 633 (1941).
- [44] E. J. W. Verwey and J. T. G. Overbeek, *Theory of the Stability of Lyophobic Colloids: The Interaction of Sol Particles Having an Electric Double Layer* (Elsevier, Amsterdam, 1948).
- [45] J. Israelachvili, *Intermolecular and Surface Forces*, 3rd ed. (Academic Press, New York, 2011).
- [46] T. Kawasaki, A. Ikeda, and L. Berthier, *Thinning or thickening? Multiple rheological regimes in dense suspensions of soft particles*, EPL **107**, 28009 (2014).
- [47] G. Bossis and J. F. Brady, *The rheology of Brownian suspensions*, J. Chem. Phys. **91**, 1866 (1989).
- [48] R. Mari, R. Seto, J. F. Morris, and M. M. Denn, *Discontinuous shear thickening in Brownian suspensions by dynamic simulation*, Proc. Natl. Acad. Sci. USA **112**, 15326 (2015).
- [49] J. Happel and H. Brenner, *Low Reynolds number hydrodynamics —with special applications to particulate media—* (Noordhoff International Publishing, Leiden, 1973).
- [50] D. J. Jeffrey and Y. Onishi, *Calculation of the resistance and mobility functions for two unequal rigid spheres in low-Reynolds-number flow*, J. Fluid Mech. **139**, 261 (1984).
- [51] D. J. Jeffrey, *The calculation of the low Reynolds number resistance functions for two unequal spheres*, Phys. Fluids A **4**, 16 (1992).
- [52] S. Kim and S. J. Karrila, *Microhydrodynamics: Principles and Selected Applications* (Dover, New York, 2005).
- [53] K. Ichiki, A. E. Kobryn, and A. Kovalenko, *Resistance functions for two unequal spheres in linear flow at low Reynolds number with the Navier slip boundary condition* arXiv:1302.0461.
- [54] Our description of the motion of the particles can have an inertial term inserted via Newton's equations. Inclusion of the inertial terms has a practical advantage, because the simulation of under-damped particles is much easier than that of over-damped particles.
- [55] See the Supplemental Material for this paper.
- [56] The expression of $A_{ij,\alpha\beta}^{(11)}$ is given by $A_{ij,\alpha\beta}^{(11)} = X_{ij}^{A(11)} \hat{k}_{ij,\alpha} \hat{k}_{ij,\beta} + Y_{ij}^{A(11)} (\delta_{\alpha\beta} - \hat{k}_{ij,\alpha} \hat{k}_{ij,\beta})$, with $\hat{k}_{12} \equiv (\mathbf{r}_2 - \mathbf{r}_1)/|\mathbf{r}_2 - \mathbf{r}_1|$, $X_{ij}^{A(11)} = (3/4)\pi d_H/h_{ij}$, and $Y_{ij}^{A(k\ell)} = (1/2)\pi d_H \ln(1/h_{ij})$, where we have introduced $h_{ij} \equiv 2(r_{ij}/d_H - 1)$ (see also the Supplemental Material [55] for the details).
- [57] The expression of $\tilde{G}_{ij,\alpha\beta\gamma}^{(11)} = G_{\beta\gamma\alpha}^{(11)}$ is given by $G_{ij,\alpha\beta\gamma}^{(11)} = X_{ij}^{G(11)} (\hat{k}_{ij,\gamma} \hat{k}_{ij,\alpha} - \frac{1}{3}\delta_{\gamma\alpha}) \hat{k}_{ij,\beta} + Y_{ij}^{G(11)} (\hat{k}_{ij,\gamma} \delta_{\alpha\beta} + \hat{k}_{ij,\alpha} \delta_{\gamma\beta} - 2\hat{k}_{ij,\gamma} \hat{k}_{ij,\alpha} \hat{k}_{ij,\beta})$, with $X_{ij}^{G(k\ell)} = (3/8)\pi d_H^2/h_{ij}$ and $Y_{ij}^{G(k\ell)} = (1/8)\pi d_H^2 \ln(1/h_{ij})$ (see also the Supplemental Material [55] for the details).
- [58] D. J. Evans and G. Morriss, *Statistical Mechanics of Nonequilibrium Liquids 2nd ed.* (Cambridge Univ. Press, Cambridge, 2008).
- [59] D. J. Evans and G. P. Morriss, *Nonlinear-response theory for steady planar Couette flow*, Phys. Rev. A **30**, 1528 (1984).
- [60] A. W. Lees and S. F. Edwards, *The computer study of transport processes under extreme conditions*, J. Phys. C: Solid State Phys. **5**, 1921 (1972).
- [61] The expressions of $G_{ij,\alpha\beta\gamma}^{(11)}$ and $M_{ij,\alpha\beta}^{(1)}$ are, respectively, given by $G_{ij,\alpha\beta\gamma}^{(11)} = \tilde{G}_{ij,\gamma\alpha\beta}^{(11)}$ and $M_{ij,\alpha\beta\gamma\delta}^{(11)} = X_{ij}^{M(11)} \hat{k}_{ij,\alpha\beta\gamma\delta}^{(0)} + Y_{ij}^{M(11)} \hat{k}_{ij,\alpha\beta\gamma\delta}^{(1)} + Z_{ij}^{M(11)} \hat{k}_{ij,\alpha\beta\gamma\delta}^{(2)}$, with $X_{ij}^{M(11)} = (1/8)\pi d_H^3/h_{ij}$, $Y_{ij}^{M(11)} = (1/10)\pi d_H^3 \ln(1/h_{ij})$, and $Z_{ij}^{M(11)} \simeq (5/6)\pi d_H^3$, where we also have introduced

- $\hat{k}_{ij,\alpha\beta\gamma\delta}^{(0)}$, $\hat{k}_{ij,\alpha\beta\gamma\delta}^{(1)}$, and $\hat{k}_{ij,\alpha\beta\gamma\delta}^{(2)}$ presented in Ref. [55].
- [62] M. L. Hunt, R. Zenit, C. S. Campbell, and C. E. Brennen, *Revisiting the 1954 suspension experiments of R. A. Bagnold*, J. Fluid Mech. **452**, 1 (2002).
 - [63] C. G. de Kruif, E. M. F. van Iersel, A. Vrij, and W. B. Russel, *Hard sphere colloidal dispersions: Viscosity as a function of shear rate and volume fraction*, J. Chem. Phys. **83**, 4717 (1985).
 - [64] G. K. Batchelor and J. T. Green, *The determination of the bulk stress in a suspension of spherical particles to order c^2* , J. Fluid Mech. **56**, 401 (1972).
 - [65] We can estimate the dimensionless softness for this system. Introducing the spring constant k in Eq. (1) as $k \equiv \varepsilon/d^2$, we get $\varepsilon^* = k/(m\zeta^2)$. The spring constant is
-

related to Young's modulus Y as $k \sim (\mathcal{A}/d)Y$, where $\mathcal{A} = \pi r_A^2$ is the area of the contact surface between two particles with the radius r_A . Thus, we rewrite ε^* as $\varepsilon^* = \mathcal{A}Y/(md\zeta^2)$. Let us evaluate \mathcal{A} . We may assume that the contact distance is evaluated as $d - d_H$, which can be approximated as $1 - \cos\theta_0 \approx \theta_0^2/2$ where θ_0 is the angle of the edge of the contact area. Thus, θ_0 can be evaluated as $\theta_0 \approx \sqrt{2\delta}$, where δ is the roughness parameter. Similarly, the radius of the contact area r_A is evaluated as $(d/2)\sin\theta_0 \approx (d/2)\theta_0 = \sqrt{2\delta}d/2$. Thus, we obtain $\mathcal{A} \approx \pi d^2\delta/2$. Substituting these values into $\varepsilon^* \sim \pi dY\delta/(m\zeta^2)$ we obtain $\varepsilon^* \sim 6 \times 10^5\delta \sim 6 \times 10^3$. This value is close to that which we used in this paper.

Supplemental Materials for “Discontinuous Shear Thickening of a Moderately Dense Inertial Suspension of Hydrodynamically Interacting Frictionless Soft Particles: Some New Findings”

This Supplemental Material explains the details of calculations that are not included in the main text. In Sect. I, we briefly explain how we generate random numbers when the resistance matrix in Eq. (5) has non-diagonal elements. In Sect. II, we summarize the hydrodynamic interaction when we consider the lubrication force between particles. In Sect. III, we check the convergence of the results depending on the strain.

I. GENERATION OF RANDOM NUMBERS OBEYING NONUNIFORM DISTRIBUTION

In this section, let us explain how we generate random numbers obeying nonuniform distribution based on Ref. [S1]. We consider a situation where the random number X_k ($k = 1, 2, \dots, 3N$) obeys

$$\langle X_k(t)X_\ell(t') \rangle = 2D_{k\ell}\delta(t-t'). \quad (\text{S1})$$

Here, X_k and $D_{k\ell}$, respectively, relates to the noise ξ_i and the resistance matrix $\overleftrightarrow{\zeta}$ as

$$\begin{bmatrix} X_{3i-2} \\ X_{3i-1} \\ X_{3i} \end{bmatrix} = \begin{bmatrix} \xi_{i,x} \\ \xi_{i,y} \\ \xi_{i,z} \end{bmatrix}, \quad (\text{S2a})$$

$$\begin{bmatrix} D_{3i-2,3j-2} & D_{3i-2,3j-1} & D_{3i-2,3j} \\ D_{3i-1,3j-2} & D_{3i-1,3j-1} & D_{3i-1,3j} \\ D_{3i,3j-2} & D_{3i,3j-1} & D_{3i,3j} \end{bmatrix} = \begin{bmatrix} \zeta_{ij,xx} & \zeta_{ij,xy} & \zeta_{ij,xz} \\ \zeta_{ij,yx} & \zeta_{ij,yy} & \zeta_{ij,yz} \\ \zeta_{ij,zx} & \zeta_{ij,zy} & \zeta_{ij,zz} \end{bmatrix}, \quad (\text{S2b})$$

for $i, j = 1, 2, \dots, N$. It is useful to introduce Y_i as

$$X_k = \sum_{\ell=1}^k \alpha_{k\ell} Y_\ell, \quad (\text{S3})$$

where Y_k satisfies

$$\langle Y_k(t) \rangle = 0, \quad \langle Y_k(t)Y_\ell(t') \rangle = 2\delta_{k\ell}\delta(t-t'). \quad (\text{S4})$$

Now, the coefficients $\alpha_{k\ell}$ should be given by (see Ref. [S1])

$$\alpha_{11} = D_{11}^{1/2}, \quad (\text{S5a})$$

$$\alpha_{k1} = D_{k1}/\alpha_{11}, \quad (\text{S5b})$$

$$\alpha_{kk} = \left(D_{kk} - \sum_{\ell=1}^{k-1} \alpha_{k\ell}^2 \right)^{1/2} \quad (k > 1), \quad (\text{S5c})$$

$$\alpha_{k\ell} = \left(D_{k\ell} - \sum_{m=1}^{\ell-1} \alpha_{km}\alpha_{\ell m} \right) / \alpha_{\ell\ell} \quad (k > \ell > 1). \quad (\text{S5d})$$

By solving Eqs. (S5) with Eq. (S3), we can evaluate the random force ξ_i .

II. HYDRODYNAMIC INTERACTION

In this section, we summarize the hydrodynamic interactions between suspended particles when the fluid motion is expressed as the Stokes equation [S2–S6]. If two particles (i -th and j -th particles, $i \neq j$) interact with each other, the following lubrication forces and stresses act between them:

$$\begin{bmatrix} \mathbf{F}_{ij}^{\text{H}} \\ \mathbf{F}_{ji}^{\text{H}} \\ \overleftrightarrow{\sigma}_{ij}^{\text{H}} \\ \overleftrightarrow{\sigma}_{ji}^{\text{H}} \end{bmatrix} = -\eta_0 \begin{bmatrix} \overleftrightarrow{A}_{ij}^{(11)} & \overleftrightarrow{A}_{ij}^{(12)} & \overleftrightarrow{G}_{ij}^{(11)} & \overleftrightarrow{G}_{ij}^{(12)} \\ \overleftrightarrow{A}_{ij}^{(21)} & \overleftrightarrow{A}_{ij}^{(22)} & \overleftrightarrow{G}_{ij}^{(21)} & \overleftrightarrow{G}_{ij}^{(22)} \\ \overleftrightarrow{G}_{ij}^{(11)} & \overleftrightarrow{G}_{ij}^{(12)} & \overleftrightarrow{M}_{ij}^{(11)} & \overleftrightarrow{M}_{ij}^{(12)} \\ \overleftrightarrow{G}_{ij}^{(21)} & \overleftrightarrow{G}_{ij}^{(22)} & \overleftrightarrow{M}_{ij}^{(21)} & \overleftrightarrow{M}_{ij}^{(22)} \end{bmatrix} \begin{bmatrix} \mathbf{v}_i - \overleftrightarrow{E} \mathbf{x}_i \\ \mathbf{v}_j - \overleftrightarrow{E} \mathbf{x}_j \\ -\overleftrightarrow{E} \\ -\overleftrightarrow{E} \end{bmatrix}, \quad (\text{S6})$$

where \mathbf{F}_{ij}^H is the force acting on i -th particle due to the lubrication effect between i -th and j -th particles. Because we are only interested in the simple shear condition, the matrix \overleftrightarrow{E} is reduced to

$$E_{\alpha\beta} = \dot{\gamma} \delta_{\alpha x} \delta_{\beta y}, \quad (\text{S7})$$

where $\dot{\gamma}$ is the shear rate.

It is known that the coefficients $A_{ij,\alpha\beta}^{(k\ell)}$, $G_{ij,\alpha\beta\gamma}^{(k\ell)}$, and $M_{ij,\alpha\beta\gamma\delta}^{(k\ell)}$ in Eq. (S6) satisfy the following symmetries [S5]:

$$A_{ij,\alpha\beta}^{(k\ell)} = A_{ij,\beta\alpha}^{(\ell k)}, \quad (\text{S8a})$$

$$G_{ij,\alpha\beta\gamma}^{(k\ell)} = \tilde{G}_{ij,\gamma\alpha\beta}^{(\ell k)}, \quad (\text{S8b})$$

$$M_{ij,\alpha\beta\gamma\delta}^{(k\ell)} = M_{ij,\gamma\delta\alpha\beta}^{(\ell k)}. \quad (\text{S8c})$$

The explicit forms of the coefficients are written as

$$A_{ij,\alpha\beta}^{(k\ell)} = X_{ij}^{A(k\ell)} \hat{k}_{ij,\alpha} \hat{k}_{ij,\beta} + Y_{ij}^{A(k\ell)} \left(\delta_{\alpha\beta} - \hat{k}_{ij,\alpha} \hat{k}_{ij,\beta} \right), \quad (\text{S9a})$$

$$G_{ij,\alpha\beta\gamma}^{(k\ell)} = X_{ij}^{G(k\ell)} \left(\hat{k}_{ij,\alpha} \hat{k}_{ij,\beta} - \frac{1}{3} \delta_{\alpha\beta} \right) \hat{k}_{ij,\gamma} + Y_{ij}^{G(k\ell)} \left(\hat{k}_{ij,\alpha} \delta_{\beta\gamma} + \hat{k}_{ij,\beta} \delta_{\alpha\gamma} - 2 \hat{k}_{ij,\alpha} \hat{k}_{ij,\beta} \hat{k}_{ij,\gamma} \right), \quad (\text{S9b})$$

$$M_{ij,\alpha\beta\gamma\delta}^{(k\ell)} = X_{ij}^{M(k\ell)} \hat{k}_{ij,\alpha\beta\gamma\delta}^{(0)} + Y_{ij}^{M(k\ell)} \hat{k}_{ij,\alpha\beta\gamma\delta}^{(1)} + Z_{ij}^{M(k\ell)} \hat{k}_{ij,\alpha\beta\gamma\delta}^{(2)}, \quad (\text{S9c})$$

respectively, where we have introduced $X_{ij}^{A(k\ell)}$, $Y_{ij}^{A(k\ell)}$, $X_{ij}^{G(k\ell)}$, $Y_{ij}^{G(k\ell)}$, $X_{ij}^{M(k\ell)}$, $Y_{ij}^{M(k\ell)}$, and $Z_{ij}^{M(k\ell)}$ which are functions of the separation length $h_{ij} \equiv 2(r_{ij} - d_H)/d_H = 2(r_{ij}/d_H - 1)$, as well as $\hat{k}_{ij,\alpha\beta\gamma\delta}^{(0)}$, $\hat{k}_{ij,\alpha\beta\gamma\delta}^{(1)}$, and $\hat{k}_{ij,\alpha\beta\gamma\delta}^{(2)}$ as [S5]

$$\hat{k}_{ij,\alpha\beta\gamma\delta}^{(0)} \equiv \frac{3}{2} \left(\hat{k}_{ij,\alpha} \hat{k}_{ij,\beta} - \frac{1}{3} \delta_{\alpha\beta} \right) \left(\hat{k}_{ij,\gamma} \hat{k}_{ij,\delta} - \frac{1}{3} \delta_{\gamma\delta} \right), \quad (\text{S10a})$$

$$\hat{k}_{ij,\alpha\beta\gamma\delta}^{(1)} \equiv \frac{1}{2} \left(\hat{k}_{ij,\alpha} \hat{k}_{ij,\gamma} \delta_{\beta\delta} + \hat{k}_{ij,\beta} \hat{k}_{ij,\gamma} \delta_{\alpha\delta} + \hat{k}_{ij,\alpha} \hat{k}_{ij,\delta} \delta_{\beta\gamma} + \hat{k}_{ij,\beta} \hat{k}_{ij,\delta} \delta_{\alpha\gamma} - 4 \hat{k}_{ij,\alpha} \hat{k}_{ij,\beta} \hat{k}_{ij,\delta} \hat{k}_{ij,\gamma} \right), \quad (\text{S10b})$$

$$\begin{aligned} \hat{k}_{ij,\alpha\beta\gamma\delta}^{(2)} \equiv & \frac{1}{2} \left(\delta_{\alpha\gamma} \delta_{\beta\delta} + \delta_{\alpha\delta} \delta_{\beta\gamma} - \delta_{\alpha\beta} \delta_{\gamma\delta} + \hat{k}_{ij,\alpha} \hat{k}_{ij,\beta} \delta_{\gamma\delta} + \hat{k}_{ij,\gamma} \hat{k}_{ij,\delta} \delta_{\alpha\beta} - \hat{k}_{ij,\alpha} \hat{k}_{ij,\gamma} \delta_{\beta\delta} \right. \\ & \left. - \hat{k}_{ij,\beta} \hat{k}_{ij,\gamma} \delta_{\alpha\delta} - \hat{k}_{ij,\alpha} \hat{k}_{ij,\delta} \delta_{\beta\gamma} - \hat{k}_{ij,\beta} \hat{k}_{ij,\delta} \delta_{\alpha\gamma} + \hat{k}_{ij,\alpha} \hat{k}_{ij,\beta} \hat{k}_{ij,\delta} \hat{k}_{ij,\gamma} \right), \end{aligned} \quad (\text{S10c})$$

When we consider their leading terms for h_{ij} , these coefficients for the monodisperse particles are reduced to [S3, S4]. Note that these expressions are dimensional. We should be careful when we compare these results with those given in Refs. [S3–S5].

$$X_{ij}^{A(11)} = -X_{ij}^{A(12)} = -X_{ij}^{A(21)} = X_{ij}^{A(22)} = 3\pi d_H \frac{1}{4} \frac{1}{h_{ij}}, \quad (\text{S11a})$$

$$Y_{ij}^{A(11)} = -Y_{ij}^{A(12)} = -Y_{ij}^{A(21)} = Y_{ij}^{A(22)} = 3\pi d_H \frac{1}{6} \ln \frac{1}{h_{ij}}, \quad (\text{S11b})$$

$$X_{ij}^{G(11)} = -X_{ij}^{G(12)} = X_{ij}^{G(21)} = -X_{ij}^{G(22)} = \frac{3}{8} \pi d_H^2 \frac{1}{h_{ij}}, \quad (\text{S11c})$$

$$Y_{ij}^{G(11)} = -Y_{ij}^{G(12)} = Y_{ij}^{G(21)} = -Y_{ij}^{G(22)} = \frac{1}{8} \pi d_H^2 \ln \frac{1}{h_{ij}}, \quad (\text{S11d})$$

$$X_{ij}^{M(11)} = X_{ij}^{M(12)} = X_{ij}^{M(21)} = X_{ij}^{M(22)} = \frac{1}{8} \pi d_H^3 \frac{1}{h_{ij}}, \quad (\text{S11e})$$

$$Y_{ij}^{M(11)} = Y_{ij}^{M(22)} = \frac{1}{10} \pi d_H^3 \ln \frac{1}{h_{ij}}, \quad Y_{ij}^{M(12)} = Y_{ij}^{M(21)} = \frac{1}{40} \pi d_H^3 \ln \frac{1}{h_{ij}}, \quad (\text{S11f})$$

$$Z_{ij}^{M(11)} = Z_{ij}^{M(22)} \simeq \frac{5}{6} \pi d_H^3, \quad Z_{ij}^{M(12)} = Z_{ij}^{M(21)} \simeq -\frac{3}{16} \pi d_H^3, \quad (\text{S11g})$$

respectively.

Let us introduce the peculiar velocity \mathbf{V}_i as

$$\mathbf{V}_i \equiv \mathbf{v}_i - \overleftrightarrow{E} \mathbf{x}_i. \quad (\text{S12})$$

Then, the force acting on i -th particle from j -th particle is given by

$$\mathbf{F}_{ij}^H = -\eta_0 \left(\overleftrightarrow{A_{ij}^{(11)}} \mathbf{V}_i + \overleftrightarrow{A_{ij}^{(12)}} \mathbf{V}_j \right) + \eta_0 \left(\overleftrightarrow{G_{ij}^{(11)}} + \overleftrightarrow{G_{ij}^{(12)}} \right) \overleftrightarrow{E}, \quad (\text{S13})$$

or equivalently,

$$\begin{aligned} F_{ij,\alpha}^H &= -\eta_0 \left(A_{ij,\alpha\beta}^{(11)} V_{i,\beta} + A_{ij,\alpha\beta}^{(12)} V_{j,\beta} \right) + \eta_0 \left(\tilde{G}_{ij,\alpha\beta\gamma}^{(11)} + \tilde{G}_{ij,\alpha\beta\gamma}^{(12)} \right) E_{\beta\gamma} \\ &= -\eta_0 \left(A_{ij,\alpha\beta}^{(11)} V_{i,\beta} + A_{ij,\alpha\beta}^{(12)} V_{j,\beta} \right) + \eta_0 \left(G_{ij,\beta\gamma\alpha}^{(11)} + G_{ij,\beta\gamma\alpha}^{(21)} \right) E_{\beta\gamma} \\ &= -\eta_0 \left(A_{ij,\alpha\beta}^{(11)} V_{i,\beta} + A_{ij,\alpha\beta}^{(12)} V_{j,\beta} \right) + 2\eta_0 \dot{\gamma} G_{ij,xy\alpha}^{(11)}, \end{aligned} \quad (\text{S14})$$

where we have used the symmetric property of the tensor $G_{ij}^{(k\ell)}$ (see Eq. (S8b)). We can rewrite $F_{ij,\alpha}^H$ furthermore. With the aid of the identity

$$\begin{aligned} A_{ij,\alpha\beta}^{(11)} V_{i,\beta} + A_{ij,\alpha\beta}^{(12)} V_{j,\beta} &= A_{ij,\alpha\beta}^{(11)} V_{i,\beta} - A_{ij,\alpha\beta}^{(11)} V_{j,\beta} \\ &= A_{ij,\alpha\beta}^{(11)} V_{ij,\beta}, \end{aligned} \quad (\text{S15})$$

with $\mathbf{V}_{ij} \equiv \mathbf{V}_i - \mathbf{V}_j$, we can rewrite Eq. (S14) as

$$F_{ij,\alpha}^H = -\eta_0 A_{ij,\alpha\beta}^{(11)} V_{ij,\beta} + 2\eta_0 \dot{\gamma} G_{ij,xy\alpha}^{(11)}. \quad (\text{S16})$$

Similarly, $F_{ji,\alpha}$ is also written as

$$\begin{aligned} F_{ji,\alpha}^H &= \eta_0 A_{ij,\alpha\beta}^{(22)} V_{ij,\beta} - 2\eta_0 \dot{\gamma} G_{ij,xy\alpha}^{(11)} \\ &= \eta_0 A_{ij,\alpha\beta}^{(11)} V_{ij,\beta} - 2\eta_0 \dot{\gamma} G_{ij,xy\alpha}^{(11)} \\ &= -F_{ij,\alpha}^H. \end{aligned} \quad (\text{S17})$$

Next, let us calculate the hydrodynamic stress tensor $\overleftrightarrow{\sigma}_{ij}^H$:

$$\begin{aligned} \overleftrightarrow{\sigma}_{ij,\alpha\beta}^H &= -\eta_0 \left(G_{ij,\alpha\beta\gamma}^{(11)} V_{i,\gamma} + G_{ij,\alpha\beta\gamma}^{(12)} V_{j,\gamma} \right) + \eta_0 \left(M_{ij,\alpha\beta\gamma\delta}^{(11)} + M_{ij,\alpha\beta\gamma\delta}^{(12)} \right) E_{\gamma\delta} \\ &= -\eta_0 \left(G_{ij,\alpha\beta\gamma}^{(11)} V_{i,\gamma} + G_{ij,\alpha\beta\gamma}^{(12)} V_{j,\gamma} \right) + \eta_0 \dot{\gamma} \left(M_{ij,\alpha\beta xy}^{(11)} + M_{ij,\alpha\beta xy}^{(12)} \right). \end{aligned} \quad (\text{S18})$$

Using the similar procedure as that in $F_{i,\alpha}$, we obtain the followings:

$$\begin{aligned} G_{ij,\alpha\beta\gamma}^{(11)} V_{i,\gamma} + G_{ij,\alpha\beta\gamma}^{(12)} V_{j,\gamma} &= G_{ij,\alpha\beta\gamma}^{(11)} V_{i,\gamma} - G_{ij,\alpha\beta\gamma}^{(11)} V_{j,\gamma} \\ &= G_{ij,\alpha\beta\gamma}^{(11)} V_{ij,\gamma}. \end{aligned} \quad (\text{S19})$$

and

$$\begin{aligned} M_{ij,\alpha\beta xy}^{(11)} + M_{ij,\alpha\beta xy}^{(12)} &= (X_{11}^M + X_{12}^M) \hat{k}_{\alpha\beta xy}^{(0)} + (Y_{11}^M + Y_{12}^M) \hat{k}_{\alpha\beta xy}^{(1)} + (Z_{11}^M + Z_{12}^M) \hat{k}_{\alpha\beta xy}^{(2)} \\ &= M_{ij,\alpha\beta}^{(1)}, \end{aligned} \quad (\text{S20})$$

where we have introduced

$$M_{ij,\alpha\beta}^{(1)} \equiv X_{ij}^{M(1)} \hat{k}_{ij,\alpha\beta xy}^{(0)} + Y_{ij}^{M(1)} \hat{k}_{ij,\alpha\beta xy}^{(1)} + Z_{ij}^{M(1)} \hat{k}_{ij,\alpha\beta xy}^{(2)}, \quad (\text{S21})$$

with

$$X_{ij}^{M(1)} \equiv X_{ij}^{M(11)} + X_{ij}^{M(12)} = \frac{1}{4} \pi d_H^3 \frac{1}{h_{ij}}, \quad (\text{S22a})$$

$$Y_{ij}^{M(1)} \equiv Y_{ij}^{M(11)} + Y_{ij}^{M(12)} = \frac{1}{8} \pi d_H^3 \ln \frac{1}{h_{ij}}, \quad (\text{S22b})$$

$$Z_{ij}^{M(1)} \equiv Z_{ij}^{M(11)} + Z_{ij}^{M(12)} = \frac{31}{48} \pi d_H^3. \quad (\text{S22c})$$

Then, we can evaluate $\overleftrightarrow{\sigma}_{ij}^H$ as

$$\overline{\sigma}_{ij,\alpha\beta}^H = -\eta_0 G_{ij,\alpha\beta\gamma}^{(11)} V_{ij,\gamma} + \eta_0 \dot{\gamma} M_{ij,\alpha\beta}^{(1)}. \quad (\text{S23})$$

We can also calculate $\overleftrightarrow{\sigma}_{ji}^H$, whose $\alpha\beta$ component is given by

$$\overline{\sigma}_{ji,\alpha\beta}^H = -\eta_0 \left(G_{ij,\alpha\beta\gamma}^{(21)} V_{i,\gamma} + G_{ij,\alpha\beta\gamma}^{(22)} V_{j,\gamma} \right) + \eta_0 \dot{\gamma} \left(M_{ij,\alpha\beta xy}^{(21)} + M_{ij,\alpha\beta xy}^{(22)} \right), \quad (\text{S24})$$

where

$$G_{ij,\alpha\beta\gamma}^{(21)} V_{i,\gamma} + G_{ij,\alpha\beta\gamma}^{(22)} V_{j,\gamma} = -G_{ij,\alpha\beta\gamma}^{(22)} V_{ij,\gamma}, \quad (\text{S25})$$

and

$$M_{ij,\alpha\beta}^{(2)} \equiv X_{ij}^{M(2)} \widehat{k}_{ij,\alpha\beta xy}^{(0)} + Y_{ij}^{M(2)} \widehat{k}_{ij,\alpha\beta xy}^{(1)} + Z_{ij}^{M(2)} \widehat{k}_{ij,\alpha\beta xy}^{(2)}, \quad (\text{S26})$$

with

$$X_{ij}^{M(2)} \equiv X_{ij}^{M(21)} + X_{ij}^{M(22)} = X_{ij}^{M(1)}, \quad (\text{S27a})$$

$$Y_{ij}^{M(2)} \equiv Y_{ij}^{M(21)} + Y_{ij}^{M(22)} = Y_{ij}^{M(1)}, \quad (\text{S27b})$$

$$Z_{ij}^{M(2)} \equiv Z_{ij}^{M(21)} + Z_{ij}^{M(22)} = Z_{ij}^{M(1)}. \quad (\text{S27c})$$

There, the hydrodynamic stress due to the hydrodynamic interaction between i -th and j -th particles is given by

$$\begin{aligned} \overline{\sigma}_{ij,\alpha\beta}^H &= \overline{\sigma}_{ij,\alpha\beta} + \overline{\sigma}_{ji,\alpha\beta} \\ &= -\eta_0 \left(G_{ij,\alpha\beta\gamma}^{(11)} - G_{ij,\alpha\beta\gamma}^{(22)} \right) V_{ij,\gamma} + \eta_0 \dot{\gamma} \left(M_{ij,\alpha\beta}^{(1)} + M_{ij,\alpha\beta}^{(2)} \right) \\ &= -2\eta_0 G_{ij,\alpha\beta\gamma}^{(11)} V_{ij,\gamma} + 2\eta_0 \dot{\gamma} M_{ij,\alpha\beta}^{(1)}. \end{aligned} \quad (\text{S28})$$

In the LF-DEM simulation, we introduce the outer-cutoff of the interaction range r_{\max} which is given by $r_{\max}/d_H = 1.5$.

III. CONVERGENCE OF THE RESULTS WITH RESPECT TO THE STRAIN INCREMENT OF THE NOISE

In this section, we verify the convergence of the results regardless of the update interval of the noise term. Although the noise term depends on the configuration of particles when the hydrodynamic interaction exists, the generation of the noise is time-consuming as compared to the case when the resistance matrix is diagonal. Thus, we need to look for the optimal update interval of the noise to implement the simulation code.

Let us check how the choice of the update step affects the results. Since we are interested in the behavior under a simple shear with $\dot{\gamma}$, the dimensionless time scale in the simulation is the strain $\gamma \equiv \dot{\gamma}t$. Therefore, the time increment in the simulation is expressed as the step strain $\Delta\gamma$ in the simulation.

Figure S1 shows that the evolution of the temperature is insensitive to the choice of the interval, at least, for $\Delta\gamma \lesssim 10^{-1}$. Therefore, in this paper, we adopt the updated interval of the noise term $\Delta\gamma = 10^{-1}$.

-
- [S1] M. P. Allen and D. J. Tildesley, *Computer Simulation of Liquids* (Oxford Univ. Press, Oxford, 1987).
[S2] J. Happel and H. Brenner, *Low Reynolds number hydrodynamics —with special applications to particulate media—* (Noordhoff International Publishing, Leiden, 1973).
[S3] D. J. Jeffrey and Y. Onishi, *Calculation of the resistance and mobility functions for two unequal rigid spheres in low-Reynolds-number flow*, J. Fluid Mech. **139**, 261 (1984).
[S4] D. J. Jeffrey, *The calculation of the low Reynolds number resistance functions for two unequal spheres*, Phys. Fluids A **4**, 16 (1992).
[S5] S. Kim and S. J. Karrila, *Microhydrodynamics: Principles and Selected Applications* (Dover, New York, 2005).
[S6] K. Ichiki, A. E. Kobryn, and A. Kovalenko, *Resistance functions for two unequal spheres in linear flow at low Reynolds number with the Navier slip boundary condition*, arXiv:1302.0461.

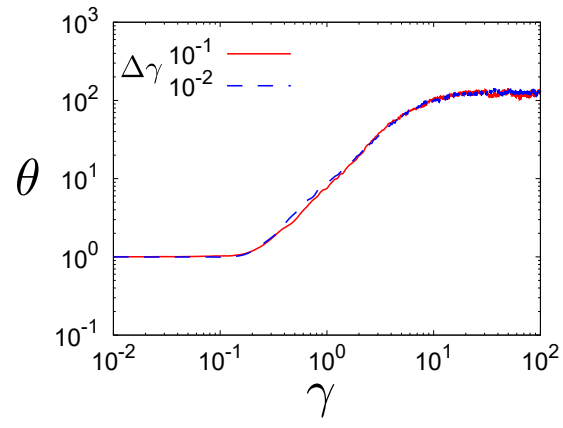


FIG. S1. Plot of θ against the strain γ for the step strain $\Delta\gamma = 10^{-1}$ (solid line) and 10^{-2} (dashed line) under the conditions of $\varphi = 0.30$, $\varepsilon^* = 10^4$, and $\xi_{\text{env}} = 1.0$.